Tertiary Structure in N-Linked Oligosaccharides†

S. W. Homans,* R. A. Dwek, and T. W. Rademacher
Department of Biochemistry, University of Oxford, Oxford OX1 3QU, England
Received March 3, 1987; Revised Manuscript Received May 21, 1987

ABSTRACT: Distance constraints derived from two-dimensional nuclear Overhauser effect measurements have been used to define the orientation of the Manα1–3Manβ linkage in seven different N-linked oligosaccharides, all containing the common pentasaccharide core Manα1–6(Manα1–3)Manβ1–4GlcNAcβ1–4GlcNAc. Conformational invariance of the Manα1–3Manβ linkage was found for those structures bearing substitutions on the Manα1–3Manβ antenna. However, the presence of either a GlcNAc residue in the β1–4 linkage to Manβ ("bisecting GlcNAc") or a xylose residue in the β1–2 linkage to Manβ of the trimannosyl core was found to generate conformational transitions that were similar. These transitions were accompanied by characteristic chemical shift perturbations of proton resonances in the vicinity of the Manα1–3Manβ linkage. Molecular orbital energy calculations suggest that the conformational transition between the unsubstituted and substituted cores arises from energetic constraints in the vicinity of the Manα1–3Manβ linkage, rather than specific long-range interactions. These data taken together with our previous results on the Manα1–6Manβ linkage [Homans, S. W., Dwek R. A., Boyd, J., Mahmoudian, M., Richards, W. G., & Rademacher, T. W. (1986) *Biochemistry 25*, 6342] allow us to discuss the consequences of the modulation of oligosaccharide solution conformations.

Most serum-derived and cell surface proteins are glycosylated (i.e., have covalently attached oligosaccharides). Although the "glyco" part has been implicated in a number of biological phenomena, its precise functional significance remains obscure. Since the constituent monosaccharides can be linked in many different ways, oligosaccharide structures are usually branched. Consequently, the potential information encoded into an oligosaccharide via its primary sequence and three-dimensional structure is considerable.

A number of studies upon oligosaccharide solution conformations have been undertaken based upon the ^{1}H NMR[1] nuclear Overhauser effect and spin-coupling constant data (Homans et al., 1982, 1983; Brisson & Carver, 1983a,b; Bock et al., 1982; Paulsen et al., 1984). As a rule, N-linked oligosaccharides contain the common pentasaccharide core:

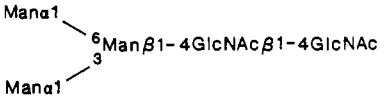

Substitutions on the α-mannosyl residues of the core give rise to the α1–6 or α1–3 antennae. Recently, we have investigated the effects of primary sequence changes upon the orientation of the Manα1–6Manβ antenna in a variety of oligosaccharides (Homans et al., 1986). The precise orientation of this antenna was found to be dependent upon key monosaccharide residues situated in both the Manα1–6Manβ antenna and the pentasaccharide core.

To further our investigation concerning the structural factors that influence the overall solution conformation of an oligosaccharide, we now investigate the effects of primary sequence modifications upon the solution conformation of the Manα1–3Manβ antenna linkages in a similar series of N-linked oligosaccharides. The structures that we have investigated (shown in Figure 1) possess a variety of substitutions on the Manα1–3Manβ antenna and the core. In this paper, we derive the necessary conditions by which quantitative distance information can be obtained in these compounds using two-dimensional nuclear Overhauser effect spectroscopy (NOESY).[1] We then use these data to generate structures that can be compared with those from theoretical predictions of the minimum energy conformer(s) about the Manα1–3Manβ linkage obtained by using molecular orbital (MNDO) methods. Finally, we discuss the possible biological relevance of the overall solution conformations adopted by the various oligosaccharide types.

Materials and Methods

The isolation of compound I from hen ovomucoid by large-scale hydrazinolysis has been described previously (Homans et al., 1984). Compound II was isolated on a Bio-Gel P-4 (–400 mesh) column (200 cm × 1.5 cm) and eluted at 8.2 glucose units after the ovomucoid oligosaccharide structures eluting at ~10.5 glucose units were digested with *Streptococcus pneumoniae* β-*N*-acetylhexosaminidase. Compounds III and VI were released from bovine pancreatic ribonuclease (Liang et al., 1980) and soybean agglutinin (Dorland et al., 1981), respectively, by large-scale hydrazinolysis, followed by purification on Bio-Gel P-4 (–400 mesh). Compound III eluted at 8.4 glucose units, and compound VI eluted at 12.3 glucose units. Compound IV was prepared by desialylation using *Arthrobacter ureafaciens* neuraminidase of the disialylated oligosaccharide obtained from human serotransferrin as described previously (Homans et al, 1983). Compound V was released from sheep immunoglobulin G by large-scale hydrazinolysis, followed by purification on a column (20 cm × 0.5 cm) of concanavalin A–Sepharose. The unbound fraction was applied to a column of Bio-Gel P-4 (–400 mesh), and compound V was isolated as the fraction eluting at 14.5 glucose units. Compound VII is a glycopeptide derived from

† This work is a contribution from the Oxford Oligosaccharide Group, which is supported by Monsanto. S.W.H., R.A.D., and T.W.R. are members of the Oxford Enzyme Group.

[1] Abbreviations: NMR, nuclear magnetic resonance; COSY, ^{1}H–^{1}H correlated spectroscopy; TQCOSY, triple quantum filtered ^{1}H–^{1}H correlated spectroscopy; NOE, nuclear Overhauser effect; NOESY, nuclear Overhauser effect spectroscopy; RECSY, relayed correlation spectroscopy; MNDO, modified neglect of diatomic differential overlap; ROESY, rotating frame Overhauser effect spectroscopy.

0006-2960/87/0426-6553$01.50/0

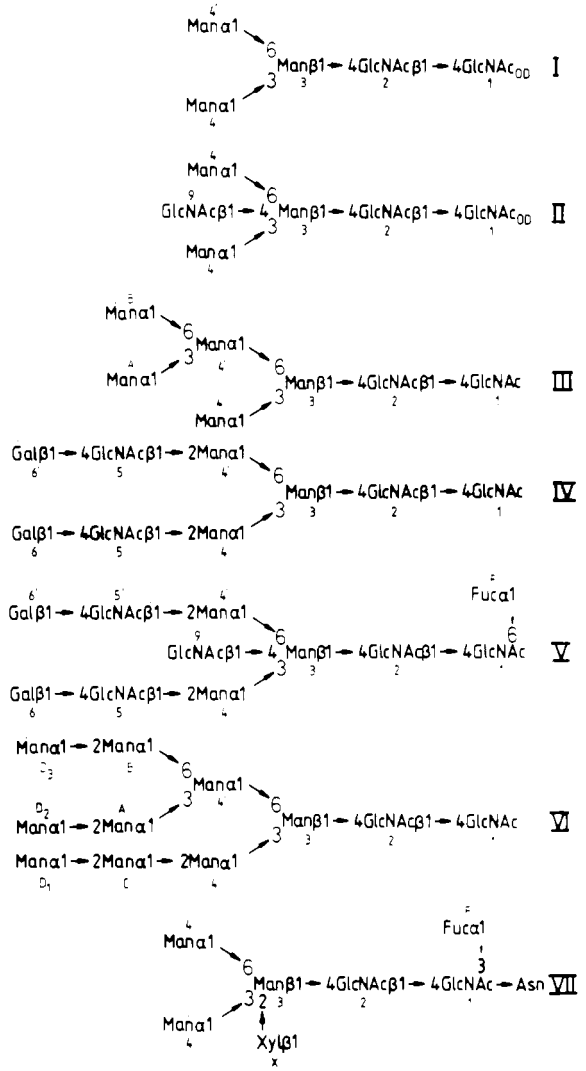

FIGURE 1: Structures of oligosaccharides described in this study. The subscript OD indicates oligosaccharides reduced with sodium borodeuteride.

the lectin of *Erythrina cristagallii* (Ashford et al., 1987), which was a gift from Professor N. Sharon (Weizmann Institute, Rehovot, Israel). Samples were prepared in deuterium oxide for NMR studies at concentrations of ~5 mM as described previously (Homans et al., 1984).

NMR Spectroscopy. Two-dimensional ^1H–^1H phase-sensitive correlated spectroscopy (COSY) was performed at 500 MHz according to Müller and Ernst (1980) and States et al. (1982) at a probe temperature of 30 °C. In total, 1024 t_1 increments of 32 scans each were recorded with a variable sweep width and 1024 real data points in t_2. The time domain data matrix was "zero-filled" once in each dimension to yield a final resolution of 2048 × 2048 real data points. Two-dimensional ^1H–^1H phase-sensitive nuclear Overhauser effect (NOESY) experiments were performed by using identical conditions to those in COSY experiments, although only 512 t_1 increments were collected. One-dimensional NOE difference spectra were recorded at 300 MHz with a probe temperature of 50 °C (Richarz & Wüthrich, 1978).

Two-dimensional rotating frame Overhauser effect spectroscopy (ROESY) was performed according to Bax and Davis (1985) with a mixing time τ_m of 500 ms at a probe temperature of 30 °C. The transmitter offset was placed at the low-field end of the spectrum to minimize coherence transfer (Hartmann–Hahn cross-speaks) between the resonances of interest.

Energy Calculations. Stable conformers of the Manα1–3Manβ linkage in the model compounds Manα1–3Manβ, Manα1–3(GlcNAcβ1–4)Manβ, Manα1–3(Xylβ1–2)Manβ, and Manα1–3Manβ1–4GlcNAcβ were determined according to molecular orbital (MNDO) procedures by complete optimization of bond lengths, bond angles, and torsional angles in each compound by use of the AMPAC molecular orbital package (Dewar & Stewart, 1986). We have previously found such methods to be superior to empirical methods in the calculation of potential surfaces in oligosaccharides (Homans et al., 1986). Ring carbon atoms in the model compounds are designated clockwise C1–C5, with C1 being the anomeric carbon. The ring oxygen is designated O5. The remaining hydrogen and oxygen atoms are labeled according to their parent carbon atoms, with hydroxyl protons designated H′. The dihedral angles about the glycosidic linkages are defined as ϕ = C1O1C3H3 and ψ = C2C1O1C3, where C3 and H3 are the aglyconic atoms. Following the molecular orbital (MNDO) optimisation, ϕ and ψ were rotated independently in 30° steps in order to locate additional low-energy conformers on the potential surface of the Manα1–3Manβ linkage. Where necessary, the torsional angles of hydroxyl groups adjacent to the Manα1–3Manβ linkage were simultaneously optimized at each stage to account for the possibility of steric hindrance to rotation about ϕ and ψ. The range of conformations that encompassed 99%, 95%, and 70% of the molecules at 37 °C was calculated by using a statistical mechanical procedure on the computed potential surface (Richards & Ganellin, 1974).

RESULTS

General resonance assignment strategies involving ^1H–^1H correlated spectroscopy (COSY), relayed correlation spectroscopy (RECSY), and triple quantum filtered COSY (TQCOSY) have been described previously for structures I–VI (Homans et al., 1986). In view of the perturbing influence of the β1–2 xylose residue, cross-peaks in the COSY spectrum of VII could be assigned without recourse to the other methods. In the present study all two-dimensional spectra were recorded sequentially and under otherwise identical experimental conditions for each of structures I–VII. Cross-peaks corresponding to intra- and interresidue NOE's could therefore by assigned in NOESY spectra (see below) by overlaying the COSY and/or RECSY and TQCOSY spectra. This approach is less time consuming in comparison with explicit assignment of each resonance and is preferable in view of the inherent inaccuracy in the measurement of chemical shift values from two-dimensional spectra at low digital resolution.

^1H–^1H Nuclear Overhauser Effects. The ring geometry of the constituent monosaccharides in each oligosaccharide studied are essentially fixed in the $^4C_1$ conformation, with the exception of L-fucose which is $^1C_4$. This is readily proven by consideration of the spin-coupling constants (J's) between adjacent protons within the ring. In order to determine the solution conformation of an oligosaccharide, therefore, it is necessary only to define ϕ and ψ for each glycosidic linkage using ^1H–^1H nuclear Overhauser effects (NOE's) (Homans et al., 1982; Brisson & Carver, 1983a,b; Book et al., 1982; Paulsen et al., 1984). In general, steady-state NOE measurements have been employed, whereby a quantitative interpretation of relative NOE's, i.e., a comparison of intraresidue vs. interresidue NOE intensities, gives distance information by virtue of the r^{-6} dependence of the NOE (where r is the internuclear distance). In the present study we employ phase-sensitive NOESY experiments for distance determination (States et al., 1982; Müller & Ernst 1980). The advantages of this method have been well documented in the context

of protein NMR (Wüthrich et al., 1982) and are of equal importance when used for NOE measurements in oligosaccharides. However, an important difference between one-dimensional saturation recovery steady-state NOE measurements and the NOESY experiment is that the latter is a *transient* method, and the magnitude of the NOE (cross-peak intensity) is not necessarily proportional to r^{-6}. In order to derive quantitative distance information, it is necessary in principle to record a series of NOESY spectra for different mixing times. Under these conditions the *initial* buildup rate of cross-peak intensities is proportional to the cross-relaxation rate between the two nuclei (σ) and thus also to r^{-6}. However, provided the initial buildup rate is linear, quantitative distance information can be obtained to good accuracy by means of the approximate relationship:

$$r_{IS}/r_{IM} \simeq (a_{IM}/a_{IS})^{1/6} \quad (1)$$

where for a three-spin system ISM, the r's correspond to the internuclear distances, the a's correspond to the cross-peak intensities, and r_{IS}, for example, is a known internuclear distance. The importance of eq 1 is that, provided τ_m is chosen within the linear region of the initial buildup rate, quantitative distance information is available from a NOESY experiment with a *single* mixing time, τ_m (Clore & Gronenborn, 1985).

In view of the large time requirement for a single NOESY experiment, the derivation of a suitable value of τ_m for each oligosaccharide is prohibitively time consuming. We therefore use oligosaccharide VI as a model. Since it is one of the largest structures investigated, it is reasonable to assume that the rotational correlation time and thus the cross-relaxation rates will correspondingly be relatively large. The initial rate approximation will therefore be violated more rapidly with respect to the mixing time in this structure, and a suitable value of τ_m can be used with confidence to ensure the validity of eq 1 in structures I–V and VII. A further advantage in using structure VI as a model is that Man-3 H3 and H4 are not strongly coupled, a situation which otherwise complicates the interpretation of interresidue NOE's in structures I–IV and VII (see below).

The time dependence of the intraresidue NOE between Man-4 H1 and Man-4 H2 in structure VI is shown in Figure 2, together with the time dependencies of interresidue NOE's connecting Man-4 H1 to Man-3 H2 and Man-4 H1 to Man-3 H3. We find that the buildup rate of the NOE connecting Man-4 H1 to Man-3 H3 is approximately linear between τ_m = 0 and τ_m = 250 ms. As is usual with NOESY experiments, the optimum mixing time is a compromise between reasonable signal-to-noise ratio in the cross sections and nonviolation of the initial rate approximation. With due consideration to each of these requirements a mixing time of 250 ms would appear to be near optimal. In practice, we find it convenient to record NOESY spectra with τ_m = 250 ms and τ_m = 700 ms for each compound. The larger mixing time allows for a *qualitative* interpretation of long-range and relayed (three-spin) NOE's which have a very slow time development.

Solution Conformation about Manα1–3Manβ Linkage in Structure VI. The buildup rates of the interresidue NOE's shown in Figure 2 provide quantitative distance information across the Manα1–3Manβ glycosidic linkage in structure VI. By measurement of relative cross-peak intensities in cross sections through the NOESY spectrum for τ = 250 ms, these distances could be defined by using eq 1, where the intraresidue NOE linking Man-4 H1 to Man-4 H2 was referenced to the corresponding internuclear distance measured from the MNDO optimized structure of Manα1–3Manβ1–4GlcNAcβ (see below and Table I). In addition, an interresidue NOE

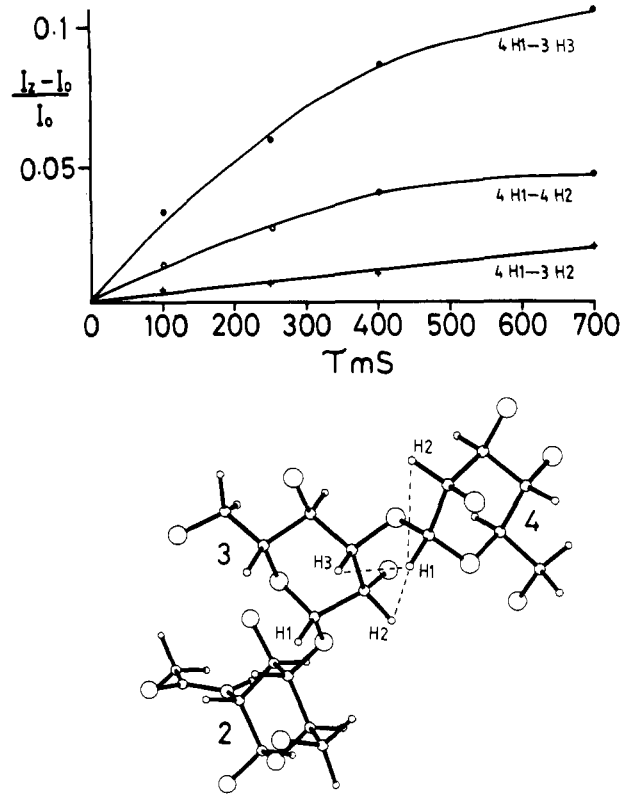

FIGURE 2: Time dependence of NOE cross-peaks in cross sections through NOESY spectra of structure VI with Man-4 H1 on the diagonal ($\omega_2 = \omega_1$ = 5.33 ppm). The curves correspond with the following NOE's, which are illustrated on the ball-and-stick model (hydroxyl protons omitted for clarity): (●) Man-4 H1 to Man-3 H3; (○) Man-4 H1 to Man-4 H2; (+) Man-4 H1 to Man-3 H2.

from Man-3 H2 to Man-4 H1 was measurable, which provided a check on the symmetry of the cross-relaxation pathway between Man-3 H2 and Man-4 H1. The relevant parameters are shown in Table I, together with the computed values of ϕ and ψ determined from the imposed distance constraints.

In order to determine whether the experimentally derived conformer in compound VI was consistent with a minimum-energy structure, molecular orbital (MNDO) calculations were performed upon the model compounds Manα1–3Manβ and Manα1–3Manβ1–4GlcNAcβ. First, the bond lengths, bond angles, and dihedral angles in Manα1–3Manβ1–4GlcNAcβ were simultaneously optimized to generate a structure with all these parameters in the global minimum-energy configuration. The computed values of ϕ, ψ in the global minimum-energy structure are given in Table I. A more detailed calculation was then performed by varying ϕ and ψ independently in 30° steps to generate a two-dimensional potential surface for the Manα1–3Manβ linkage. The torsion angle H′4O4C4C5 was simultaneously optimized to account for steric hindrance by the hydroxyl group at C4 of Manβ. The result is illustrated in Figure 3a. The experimentally derived values for ϕ and ψ (Table I) are clearly similar to their theoretical minimum-energy values. The potential surface for Manα1–3Manβ (not shown) was not significantly different, indicating that the terminal GlcNAc residue has a negligible influence upon the orientation of the Manα1–3Manβ linkage.

We should note that for a structure similar to VI, others have derived somewhat different values for ϕ, ψ at the Manα1–3Manβ linkage (Brisson & Carver, 1983a). Importantly, these values (ϕ = −10°, ψ = −173°) generate *qualitatively* similar NOE connectivities to those described above, in that Man–4 H1 is in close proximity to Man–3 H3. The smaller NOE between Man-4 H1 and Man-3 H2 is then

Table I: NOE's, Computed Distances, and ϕ, ψ Values for the Manα1–3Manβ Linkage in Structures I–VII

structure	NOE connectivity	rel magnitude	distance (Å)	ϕ (deg), ψ (deg)
I	4-H1, 4-H2	1	2.62	
	4-H1, 3-H2	0.38	3.08	
	4-H1, 3-H3/H4	4.0[b]	2.08	+30, −140[a] +50, −140[c]
	3-H2, 3-H1	1.0	2.53	
	3-H2, 4-H1	0.38	2.97	
II	ND[d]			−15, −160[a] −5, −160[c]
III	4-H1, 4-H2	1.0	2.62[e]	
	4-H1, 3-H2	0.38	3.07[e]	
	4-H1, 3-H3/H4	4.0	2.08[e]	+30, −140 +50, −140[c]
	3-H2, 3-H1	1.0	2.53	
	3-H2, 4-H1	0.32	3.06	
IV	4-H1, 4-H2	1.0	2.62	
	4-H1, 3-H2	0.38	3.08	
	4-H1, 3-H3/H4	4.1	2.07	+30, −140[a] +50, −140[c]
	3-H2, 3-H1	1.0	2.53	
	3-H2, 4-H1	0.36	3.00	
V	4-H1, 4-H2	1.0	2.64	
	4-H1, 3-H3	2.56	2.26	−15, −160[a] −5, −160[c]
	3-H2, 3-H3	1.0	2.49	
	3-H2, 4-H5	0.67	2.66	
VI	4-H1, 4-H2	1.0	2.62	
	4-H1, 3-H2	0.4	3.05	
	4-H1, 3-H3	4.0	2.08	+30, −140[a] +50, −140[c]
	3-H2, 3-H1	1.0	2.53	
	3-H2, 4-H1	0.34	3.03	
	(3-H2, 4-H5	*f*	3.51)	see text
	(3-H2, 3-H3	1.1	2.49)	
VII	4-H1, 4-H2	1	2.64	
	4-H1, 3-H3/H4	2.7	2.24	−15, −160[a] +5, −160[c]
	3-H2, 3-H3	1	2.49	
	3-H2, 4-H5	0.65	2.67	

[a] Experimental values; we estimate an error of ±0.1 Å in the distance measurements, giving a variable error in the measurement of ϕ, ψ that is <±15°. In the case of structure VII, the error is estimated as ±30°. [b] NOE's to Man-3 H3/H4 were calculated from the total integrated intensity of the complex multiplet. [c] Theoretical values. [d] ND, not determined. [e] Approximate values due to resonance overlap of Man-4 H1 with Man-A H1. [f] Unmeasurable.

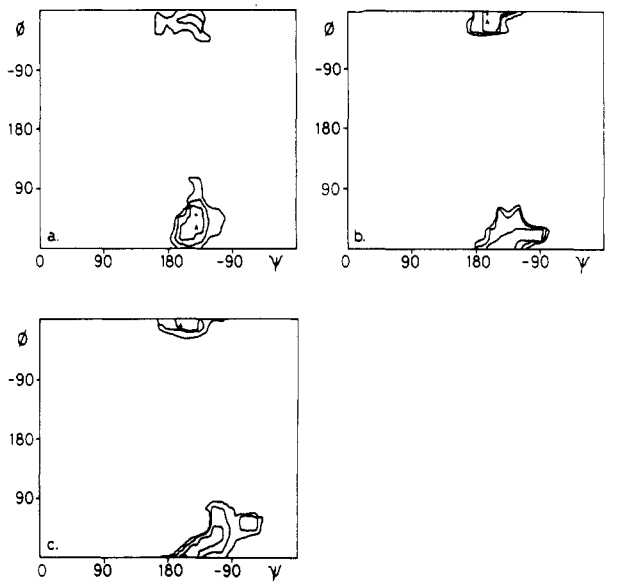

FIGURE 3: Potential surfaces for the Manα1–3Manβ linkage in (a) Manα1–3Manβ1–4GlcNAcβ, (b) Manα1–3(GlcNAcβ1–4)Manβ, and (c) Manα1–3(Xylβ1–2)Manβ, calculated by using MNDO procedures described in the text. Each surface is contoured at the energy bounds for 70%, 95%, and 99% of the molecules at 37° according to a statistical mechanical procedure (Richards & Ganellin, 1974). The experimental and theoretical minimum-energy values are denoted "Δ" and "+".

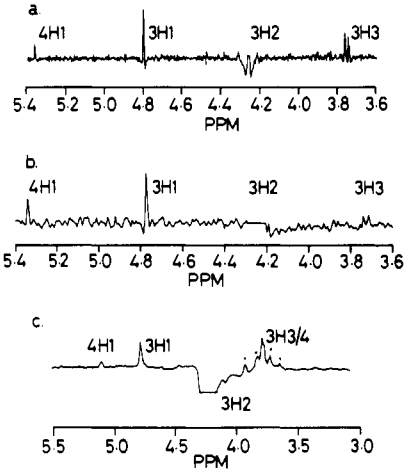

FIGURE 4: (a) Cross section through the NOESY spectrum of structure VI (τ = 700 ms) with Man-3 H2 on the diagonal. These data have been resolution enhanced with a phase-shifted sine bell function to demonstrate the presence of a clean doublet of doublets corresponding to Man-3 H3. (b) Cross section through the ROESY spectrum (τ_m = 500 ms) of structure VI with Man-3 H2 on the diagonal (negative intensity). A positive NOE linking Man-3 H2 to Man-4 H1 demonstrates that these protons are coupled by a direct (rather than relayed) mechanism. (c) The 300-MHz NOE difference spectrum of structure I obtained upon saturation of Man-3 H2. The resonances marked "." are interfering NOE's due to simultaneous saturation of terminal *N*-acetylglucosaminitol (GlcNAc-1) H2. A positive NOE linking Man-3 H2 to Man-4 H1 demonstrates that these protons are coupled by a direct (rather than relayed) mechanism. No NOE's were detected when the irradiating field was moved 30 Hz upfield from Man-3 H2 (data not shown).

generated by a relayed (three-spin) mechanism via Man-3 H3. In the present study we find that this latter conformer does not fall within the minimum-energy bounds of the potential surface (Figure 3a), and several lines of evidence indicated that it is not populated significantly in structure VI in solution. First, for ϕ, ψ = −10°, −173°, a large NOE is expected between Man-3 H2 and Man-4 H5, whereas for ϕ, ψ = +30°, −140°, this would be vanishingly small (Table I). Although this NOE could not be detected directly in complex and high-mannose type oligosaccharides in the study of Brisson and Carver (1983a), it was suggested that this was obscured due to overlap of Man-4 H5 with Man-3 H3. While our present investigations in structure VI are in agreement with those of Brisson and Carver (1983a) with regard to the resonance position of Man-4 H5 (3.79 ppm), we find no evidence for the presence of an NOE linking Man-3 H2 to Man-4 H5 in a cross section through the NOESY spectrum (τ_m = 700 ms) of VI. As shown in Figure 4a, only the pure doublet of doublets corresponding to Man-3 H3 is found. Computation of the fixed internuclear distance between Man-3 H2 and Man-3 H3 using the NOE in Figure 4a (in the absence of the apodization function) gives the expected result (Table I). In an earlier investigation in structure IV we were similarly unable to detect an NOE between Man-3 H2 and Man-4 H5, although in that study the interpretation was complicated by strong coupling between Man-3 H3 and Man-3 H4 (Homans et al., 1983).

Further evidence for the absence of the ϕ, ψ = −10°, −173° conformer in structure VI derives from the nature of the NOE linking Man-4 H1 to Man-3 H2. For ϕ, ψ = +30°, −140°, this NOE is direct, whereas for ϕ, ψ = −10°, −173°, it arises from a relayed (three-spin) effect. Under these circumstances,

it is possible in principle to distinguish between these mechanisms from the buildup rate of the NOE (Müller & Ernst, 1980). However, the poor signal-to-noise ratio of cross sections for small values of τ_m prevents the distinction of the mechanisms within experimental error. As an alternative, we have measured the relative sign of the NOE between Man-4 H1 and Man-3 H2 using rotating frame Overhauser effect spectroscopy (ROESY) (Bax & Davis, 1985). This experiment can be thought of as a technique to restore the "extreme narrowing limit" to large molecules. All direct NOE's are monotonically positive, whereas relayed NOE's are of opposite sign (Bax et al., 1986). We find that, in a cross section through the ROESY spectrum of structure VI with Man-3 H2 on the diagonal, the transverse NOE linking Man-3 H2 to Man-4 H1 is of the *same sign* as that linking Man-3 H2 to Man-3 H1, demonstrating that this NOE arises from a *direct* mechanism (Figure 4b). We consider unlikely the alternative possibility that a "false" positive NOE is generated between Man-3 H2 and Man-4 H1 due to coupled coherent and incoherent transfer pathways, since no coherence transfer (Hartmann–Hahn cross-peaks) was detected in the ROESY spectrum and cross-peaks did not exhibit pronounced offset dependence (Neuhaus & Keeler, 1986). Finally, we show below that a positive NOE is detected between Man-3 H2 and Man-4 H1 in structure I, a compound that has a rotational correlation time in the "authentic" extreme narrowing limit.

Solution Conformation of Manα1–3Manβ Linkage in Structures I, III, and IV. By analogy with the above measurements in structure VI, the distance constraints about the Manα1–3Manβ linkage derived from NOESY spectra (τ = 250 ms) of III and IV (data not shown) were found to define values for ϕ and ψ that were identical within experimental error to those found in compound VI (Table I). In addition, no significant chemical shift perturbations of resonances in the vicinity of the Manα1–3Manβ linkage were found between any of these structures, in further support of conformational invariance.

Distance constraints could not be derived for structure I by using NOESY experiments at 500 MHz, since $\omega\tau_c \sim 1$ at this frequency, resulting in unmeasurable NOE's. Therefore, steady-state saturation recovery NOE experiments were performed on structure I at 300 MHz. Under these conditions the molecule was found to possess a rotational correlation time in the extreme narrowing limit (positive NOE's). Distance constraints were calculated from NOE difference spectra according to analogous methods described for NOESY. These constraints were again found to define values for ϕ and ψ that were experimentally indistinguishable from those in structures III, IV, and VI (Table I). A small positive NOE connecting Man-3 H2 and Man-4 H1 upon saturation of the former in structure I (Figure 4c) is further evidence in support of the proposed conformer about the Manα1-3Manβ linkage in all four structures.

Solution Conformation of Manα1–3Manβ Linkage in Structure V. A cross section through the NOESY spectrum of structure V with Man-4 H1 on the diagonal shows qualitatively similar NOE's to those observed above. Conversely, a cross section with Man-3 H2 on the diagonal (Figure 5) shows an NOE between Man-3 H2 and Man-4 H5, which is not observed in structures I, III, IV, and VI. These observations are indicative of a conformational rearrangement about the Manα1–3Manβ linkage in structure V. The NOE constraints, internuclear distances, and ϕ, ψ values calculated for structure V are given in Table I. It should be noted that the NOE between Man-3 H2 and Man-4 H1 (and vice versa) in Figure 5 arises from relayed (three-spin) transfer via Man-3 H3, rather than a direct effect as observed in structures I, III, IV, and VI. As described above, this results in a *qualitative* similarity in NOE connectivities from Man-4 H1 despite the fact that the calculated values of ϕ and ψ are significantly different (Table I).

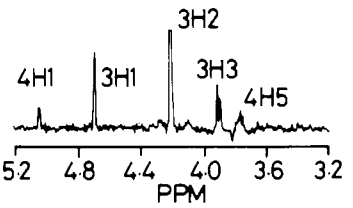

FIGURE 5: Cross section through the NOESY spectrum of structure V, with Man-3 H2 on the diagonal. Note the qualitative difference in comparison with an equivalent cross section through the NOESY spectrum of structure VI (Figure 4a).

Table II: Chemical Shifts of Protons in the Vicinity of the Manα1–3Manβ Linkage in the Structures Indicated[a]

structure	chemical shift (ppm)			
	Man-3 H2	Man-3 H3	Man-4 H1	Man-4 H2
I	4.24	3.76	5.10	4.05
II	4.18	3.90	5.21	4.14
III	4.25	3.75	5.10	4.07
IV	4.24	3.77	5.12	4.18
V	4.18	3.85	5.06	4.25
VI	4.23	3.71	5.33	4.10
VII	4.25	3.83	5.12	4.03

[a] See Figure 1 for structures.

In view of the conformational variance between structure V (ϕ, ψ = −15°, −160°) and structures I, III, IV, and VI (ϕ, ψ = +30°, −140°), chemical shift differences between protons in the vicinity of the Manα1–3Manβ linkage might be anticipated. Such differences are indeed observed and are particularly significant with respect to Man-3 H2, Man-3 H3, Man-4 H1, and Man-4 H2. Inspection of these shifts (Table II) shows that the resonance positions of Man-3 H2 and Man-3 H3 are similar in structures I, III, IV, and VI, whereas these protons are upfield and downfield shifted, respectively, in structure V. In structures I, III, IV, and VI, the ring oxygen (O5) of Man-4 is proximal to Man-3 H2 in the proposed conformation, resulting in deshielding and downfield shift. Conversely, the ring oxygen of Man-4 is proximal to Man-3 H3 as a result of the proposed conformational rearrangement in structure V, resulting in downfield shift of this proton and upfield shift of Man-3 H2. Finally, the resonance position of Man-4 H2 is downfield shifted in V due to proximity to GlcNAc-9 O5. The relevance of the chemical shift perturbations of Man-4 H1 is discussed below.

In order to determine whether the experimentally derived values of ϕ, ψ in structure V were consistent with a minimum-energy structure, a series of molecular orbital calculations were computed by using the model structure Manα1–3(GlcNAcβ1–4)Manβ. The values of ϕ, ψ about the Manα1–3Manβ linkage in this compound were varied independently in 30° steps. In order to account for possible steric hindrance due to GlcNAc-9 for certain orientations of Man-4, the dihedral angles ϕ and ψ for the former residue were optimized at each step. The resulting potential surface for rotation about the Manα1–3Manβ linkage is shown in Figure 3b. The experimentally determined values of ϕ, ψ are clearly similar to the computed minimum-energy configuration.

Solution Conformation about Manα1–3Manβ Linkage in Structure II. The rotational correlation time for structure II was such that NOE's were vanishingly small at spectrometer

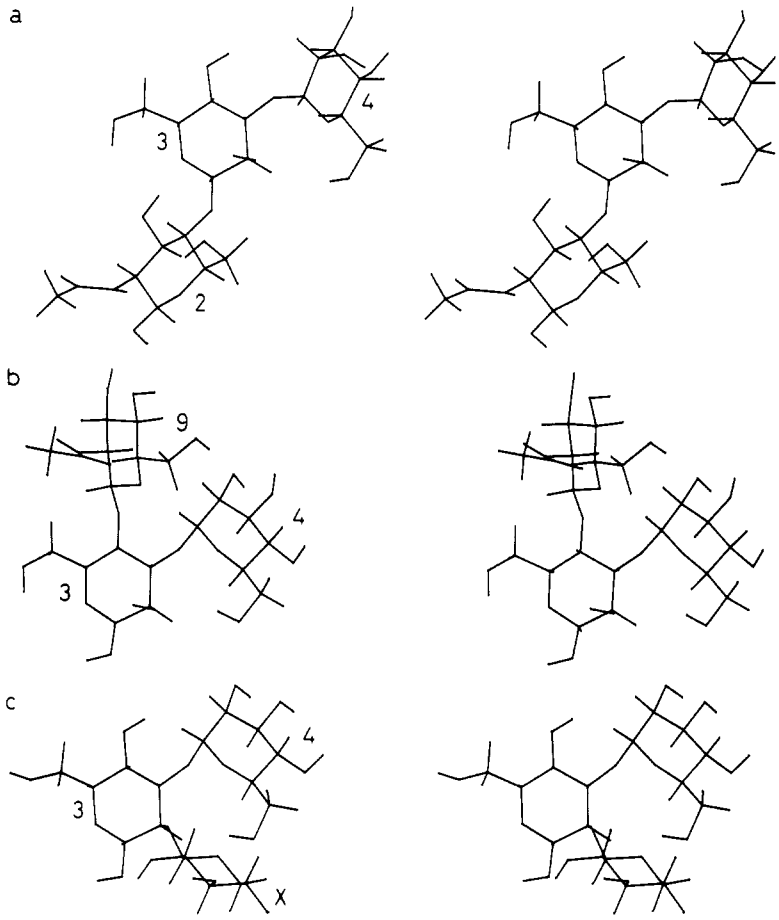

FIGURE 6: Computer-drawn stereo diagrams showing the orientation of the Manα1–3Manβ linkage in (a) Manα1–3Manβ1–4GlcNAcβ, (b) Manα1–3(GlcNAcβ1–4)Manβ, and (c) Manα1–3(Xylβ1–2)Manβ.

frequencies of both 300 and 500 MHz, and consequently quantitative distance constraints could not be obtained. However, the similarity between the characteristic chemical shift perturbations of Man-3 H2 and Man-3 H3 in structures V and II suggests that the orientation of the Manα1–3Manβ linkage is comparable in each compound (Table I). Conversely, a comparison of the chemical shifts of Man-4 H1 between the compounds with bisected and unbisected cores I and II and also between IV and V suggests subtle conformational variance of side groups in the vicinity of the Manα1-3Manβ linkage, as discussed below.

Solution Conformation about Manα1–3Manβ Linkage in Structure VII. The magnitudes of the NOE's in structure VII were small and negative. For this reason we chose to study the glycopeptide rather than the free oligosaccharide since the NOE's were unmeasurably small in the latter (data not shown). Cross sections through the NOESY spectrum of structure VII at the Larmor frequencies of Man-4 H1 and Man-3 H2 gave qualitatively similar NOE's to those found in structure V (data not shown). In particular, the presence of an NOE between Man-3 H2 and Man-4 H5 suggested that the orientation of the Manα1–3Manβ linkage in structure VII was similar to that in V. This view is supported by quantitation of the relevant NOE's, although the error in these measurements was large in comparison to that for structure V in view of their small magnitude. Further evidence for the conformational similarity in the Manα1–3Manβ linkage in structures V and VII derives from the characteristic downfield shift of Man-3 H3 in each structure. However, the shifts of Man-3 H2 and Man-4 H1 and H2 are not comparable due to the respective influence of the Xylβ1 residue in structure VII and GlcNAc-5 in structure V.

To complete the investigation of structure VII, molecular orbital calculations were computed in the model compound Manα1–3(Xylβ1–2)Manβ, to ensure that the experimentally determined values of ϕ, ψ corresponded to energy minima. For each independent 30° step in ϕ and ψ for the Manα1–3Manβ linkage in the model compound, the torsional angles about the Xylβ1–2Manβ linkage were optimized to account for possible steric hindrance to rotation due to the xylose residue. In addition, the torsional angle H'4O4C4C5 of Man-3 was simultaneously optimized to account for possible reorientation of the hydroxyl group at C4 during the rotation. The resulting potential surface for rotation about the Manα1–3Manβ linkage is shown in Figure 3c. The computed energy minimum in Manα1–3(Xylβ1–2)Manβ is similar to that obtained for Manα1–3(GlcNAcβ1–4)Manβ (Table I).

In order to illustrate the experimentally derived conformational preference of the Manα1–3Manβ linkage in the three types of core structure that we have investigated, computer-drawn diagrams of Manα1–3Manβ1–4GlcNAcβ, Manα1–3-(GlcNAcβ1–4)Manβ, and Manα1–3(Xylβ1–2)Manβ are shown in Figure 6.

Conformational Variance in Monosaccharide Residue Side Chains. In all cases described above, it was possible to rationalize chemical shift differences between the various structures in terms of the relative conformational rearrangement of monosaccharide residues, with the exception of one: Man-4 H1 is up shifted from 5.12 to 5.06 ppm when structure IV is compared with structure V but is shifted downfield from 5.10 to 5.21 ppm when structure I is compared with structure II. In terms of the proposed conformational rearrangement of the Manα1–3Manβ linkage in structure II, the downfield shift of Man-4 H1 can be rationalized in terms of its proximity

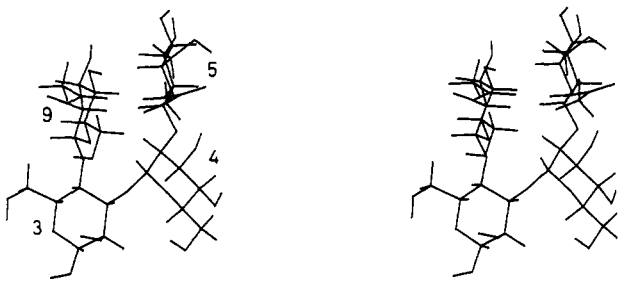

FIGURE 7: Stereo diagram to illustrate "stacking interaction" between GlcNAc-5 and GlcNAc-9 in structure V.

to Man-3 O4 and the GlcNAc-9 *N*-acetamido moiety carbonyl group. The corresponding upfield shift of Man-4 H1 in structure V can then be explained in terms of conformational rearrangement of groups in the vicinity of the Manα1–3Manβ linkage. One possibility is a conformational change about the GlcNAcβ1–2Manα linkage between structures IV and V, but this is unlikely since this linkage has been reported to have conformational invariance between these structures and no significant chemical shift perturbations occur in the vicinity of this linkage apart from Man-4 H1 (Brisson & Carver, 1983a). An alternative explanation is that the *N*-acetyl group of GlcNAc-9 undergoes a conformational rearrangement in structure V. In support of this, we note that the experimentally derived values for ϕ, ψ about the Manα1–3Manβ linkage in V allow the formation of a "stacking interaction" between GlcNAc-5 and GlcNAc-9 where a putative hydrogen bond exists between the acetamido carbonyl group of GlcNAc-9 and the H-N group of GlcNAc-5 (Figure 7).

Relevance of NMR-Derived Conformations. In the derivation of ϕ, ψ values for the Manα1–3Manβ linkage in each structure, we have interpreted the NOE constraints in terms of a single conformer. In view of the r^{-6} dependence of the NOE, an alternative interpretation that must be considered is the possibility of conformational averaging. Two lines of evidence suggest that the latter interpretation is untenable. First, the theoretical minimum-energy conformation for each structure is in a deep potential well and is in good agreement with that derived experimentally. Second, the magnitudes of the measured NOE's are close to the theoretical maximum. For example, in structure VI, the relative magnitude of the NOE linking Man-4 H1 and Man-3 H3 is 4.0, which defines an internuclear distance of 2.08 Å (Table I), whereas the distance at closest approach of Man-4 H1 and Man-3 H3 is 1.97 Å. The calculated relative magnitude of the NOE at this distance is 5.4. An alternative conformer where Man-4 H1 and Man-3 H3 are distinct would thus not be populated significantly. These considerations suggest that the NMR-derived conformation is restricted to narrow torsional excursions within the theoretical minimum-energy well. Considerations of the magnitude of these fluctuations will be the subject of a future paper (Homans et al., 1987).

Discussion

The orientation of the Manα1–3Manβ linkage in the seven structures shown in Figure 1 depends upon whether the Manα1–3(Manα1–6)Manβ1–4GlcNAcβ1–4GlcNAc core is unsubstituted or is substituted with either a β-GlcNAc residue in a 1–4 linkage or a β-xylose residue in a 1–2 linkage to the central β-mannose. The presence of either of these substitutions causes characteristic chemical shift perturbations of resonances in the vicinity of the Manα1–3Manβ linkage due to a conformation transition. In contrast, primary sequence variations distal to the Manα1–3Manβ linkage do not cause any conformational transitions in the compounds analyzed. These considerations suggest that the conformational transition between the unsubstituted and substituted cores arises from energetic constraints in the vicinity of the Manα1–3Manβ linkage, rather than specific long-range interactions. This is supported by the fact that the minimum-energy configurations in model compounds representative of unsubstituted and substituted cores are different and are in good agreement with those derived experimentally in the larger structures. These data, taken together with our previous investigations upon the conformational preference of the Manα1–6Manβ antennae in an analogous series of compounds (Homans et al., 1986), provide additional insight into the overall solution conformation(s) of a given oligosaccharide.

In our previous study (Homans et al., 1986) we presented a scheme for conformational transitions in oligosaccharides resulting from primary sequence changes. Those changes that did not alter the conformation were termed "type 1". Those that altered the conformation were designated either "type 2p" or "type 2d", depending on whether the sequence change is proximal or distal to the site of conformational variance (for example, in this study it would be the Manα1–3Manβ linkage). Part of that study involved the determination of the conformations about the Manα1–6Manβ linkage in a series of oligosaccharides following the addition of the bisecting GlcNAc. Structure V (or similar compounds) has the α1–6 antenna folded back toward the core (ω = 180°). In the absence of this substitution (e.g., in IV) the α1–6 antenna can either be extended "forward" (ω = −60°) or "folded back" (ω = 180°) due to conformational averaging about the C5–C6 bond of the Manα1–6Manβ linkage. On this basis, the overall conformation of the oligosaccharide resulting from the "bisecting" GlcNAc substitution cannot be considered unique since the resulting conformer (ω = 180°) is accessible in structures lacking this substitution.

The present study shows that the orientation of the α1–3 antenna resulting from the bisecting GlcNAc substitution generates a unique overall conformation, and in our previous nomenclature this conformer would arise from IV by a "type 2p" transition. This finding might explain the action of the erythroagglutinating phytohemagglutinin (EPHA) lectin, which specifically binds structures bearing a bisecting GlcNAc and a variety of different primary sequences on the α1–3 and α1–6 antennae (Yamashita et al., 1983). Removal of the bisecting GlcNAc *completely* abolishes binding activity, consistent with the type 2p conformational transition of the Manα1–3Manβ linkage described above. (The alternative interpretation that the lectin specifically recognizes only the bisecting GlcNAc residue is untenable since the minimum structural requirement for binding comprises the GlcNAc plus six other residues on both the α1–3 and α1–6 antennae.)

It has been proposed that the bisecting GlcNAc residue is a control point in oligosaccharide biosynthesis (Schachter, 1986). Our data suggest that the mechanism of this control lies in a conformational transition about the Manα1–3Manβ linkage rather than steric factors. Furthermore, since a similar conformational transition is generated by the xylose substitution at the 2-position of the core mannose (structure VII), we could speculate that when this substitution occurs in oligosaccharide biosynthesis (e.g., plant glycoproteins), its effect might be analogous to that of the bisecting GlcNAc substitution common in mammalian glycoproteins.

Our structural studies have shown that oligosaccharide linkages can be flexible or restricted. When attached to a protein, oligosaccharides exhibit conformations that can be

either accommodated if the appropriate conformational space is available or altered by the protein. Such an alteration in the conformations of these oligosaccharides would require an input of energy creating a "higher energy status" for the oligosaccharide. Subsequent relaxation of the imposed conformation resulting from, for example, the interaction of a receptor with a protein determinant that is distal from the oligosaccharide attachment site (Calvo & Ryan, 1985) may be important in subsequent activation events. These conformational restrictions can also directly determine the biosynthetic pathway available to the oligosaccharide (Savvidou et al., 1984). This hypothesis is supported by recent work on the influence of quaternary structure on site-specific glycosylation (Dahms & Hart, 1986).

ACKNOWLEDGMENTS

We thank Dr. A. Bax for providing a copy of a manuscript prior to publication.

Registry No. I, 70858-45-6; II, 102038-83-5; III, 66091-47-2; IV, 71496-53-2; V, 76149-64-9; VI, 71246-55-4; VII, 109929-52-4; ribonuclease, 9001-99-4.

REFERENCES

Ashford, D., Dwek, R. A., Welphy, J. K., Amatayakul, S., Homans, S. W., Lis, H., Taylor, G. N., Sharon, N., & Rademacher, T. W. (1987) *Eur. J. Biochem. 166*, 311.

Bax, A., & Davis, D. G. (1985) *J. Magn. Reson. 63*, 207.

Bax, A., Sklenar, V., & Summers, M. (1986) *J. Magn. Reson. 70*, 327.

Bock, K., Arnarp, J., & Lonngren, J. (1982) *Eur. J. Biochem. 129*, 171.

Brisson, J.-R., & Carver, J. P. (1983a) *Biochemistry 22*, 3671.

Brisson, J.-R., & Carver, J. P. (1983b) *Biochemistry 22*, 3680.

Calvo, F. O., & Ryan, R. J. (1985) *Biochemistry 24*, 1953.

Clore, G. M., & Gronenborn, A. M. (1985) *J. Magn. Reson. 61*, 158.

Dahms, N. M., & Hart, G. W. (1986) *J. Biol. Chem. 261*, 13186.

Dewar, M. J. S., & Stewart, J. J. P. (1986) AMPAC, *QCPE Bull. 506.*

Dorland, L., van Halbeek, H., Vliegenthart, J. F. G., Lis, H., & Sharon, N. (1981) *J. Biol. Chem. 256*, 7708.

Homans, S. W., Dwek, R. A., Fernandes, D. L., & Rademacher, T. W. (1982) *FEBS Lett. 150*, 503.

Homans, S. W., Dwek, R. A., Fernandes, D. L., & Rademacher, T. W. (1983) *FEBS Lett. 164*, 231.

Homans, S. W., Dwek, R. A., Fernandes, D. L., & Rademacher, T. W. (1984) *Proc. Natl. Acad. Sci. U.S.A. 81*, 6286.

Homans, S. W., Dwek, R. A., Boyd, J., Mahmoudian, M., Richards, W. G., & Rademacher, T. W. (1986) *Biochemistry 25*, 6342.

Homans, S. W., Pastore, A., Dwek, R. A., & Rademacher, T. W. (1987) *Biochemistry* (in press).

Liang, C.-J., Yamashita, K., & Kobata, A. (1980) *J. Biochem. (Tokyo) 88*, 51.

Müller, L., & Ernst, R. R. (1980) *Mol. Phys. 38*, 963.

Neuhaus, D., & Keeler, J. (1986) *J. Magn. Reson. 68*, 568.

Paulsen, H., Peters, T., Sunwell, V., Lebuhn, R., & Meyer, B. (1984) *Liebigs Ann. Chem. 5*, 951.

Richards, W. G., & Ganellin, C. R. (1974) in *Molecular and Quantum Pharmacology* (Bergman, E. D., & Pullman, B., Eds.) pp 391–400, Reidel, Dordrecht, Holland.

Richarz, R., & Wüthrich, K. (1978) *J. Magn. Reson. 30*, 147.

Savvidou, G., Klein, M., Grey, A., Dorrington, K., & Carver, J. (1984) *Biochemistry 23*, 3736.

Schachter, H. (1986) *Biochem. Cell Biol. 64*, 163.

States, D. J., Haberkorn, R. A., & Ruben, D. J. (1982) *J. Magn. Reson. 48*, 286.

Wüthrich, K., Wider, G., Wagner, G., & Braun, W. (1982) *J. Mol. Biol. 155*, 311.

Yamashita, K., Hitoi, A., & Kobata, A. (1983) *J. Biol. Chem. 258*, 14753.